Polymer-Fullerene Bulk-Heterojunction Solar Cells

By *Gilles Dennler, Markus C. Scharber,* and *Christoph J. Brabec**

Solution-processed bulk-heterojunction solar cells have gained serious attention during the last few years and are becoming established as one of the future photovoltaic technologies for low-cost power production. This article reviews the highlights of the last few years, and summarizes today's state-of-the-art performance. An outlook is given on relevant future materials and technologies that have the potential to guide this young photovoltaic technology towards the magic 10% regime. A cost model supplements the technical discussions, with practical aspects any photovoltaic technology needs to fulfil, and answers to the question as to whether low module costs can compensate lower lifetimes and performances.

1. Introduction

Solution-processed bulk-heterojunction photovoltaic cells were first reported in 1995.[1] It took another 3–4 years until the scientific community realized the huge potential of this technology, and suddenly, in 1999, the number of publications in that field started to rise exponentially. Since then, the number of publications on organic semiconductor photovoltaics has increased by about 65% per year. While the best efficiency reported eight years ago barely reached values higher than 1%, efficiencies beyond 5% are achieved today.[2–6]

This article reviews the recent developments that have guided the community and the whole field to the current performance of organic photovoltaic devices (OPVs). We start with reviewing the performance of the currently most prominent material system in OPVs, namely the mixture of poly(3-hexylthiophene):1-(3-methoxycarbonyl)propyl-1-phenyl[6,6]C_{61} (P3HT:PCBM). In the second part of this article, we discuss new and promising active materials that have already shown promising performances in actual devices, and have the potential to go to significantly higher efficiencies than those achieved by P3HT-based solar cells. The third part is devoted to the recent development of a tandem technology for the organic field. The last two sections go beyond pure advanced material science, and discuss necessary requirements to ensure that OPVs will become a sustainable technology in the market. The first part analyzes the impact of the fundamental, OPV-specific losses on the maximum theoretical efficiency, in a simplified Shockley-Queisser approach. The second part tries to answer the question of what are the minimum efficiency and lifetime a low-cost PV technology needs to demonstrate in order to become competitive for grid-connected energy supply.

Despite the great progress of several different organic/hybrid approaches, like solution-processed or evaporated small molecules, polymer–polymer blends, or organic–inorganic blends, this review will focus exclusively on bulk-heterojunction composites from polymer–fullerene blends.

[*] Dr. C. J. Brabec, Dr. G. Dennler, Dr. M. C. Scharber
Konarka Austria GmbH
Altenbergerstrasse 69
4040 Linz, Austria
E-mail: cbrabec@konarka.com

DOI: 10.1002/adma.200801283

2. The P3HT:PCBM Blend

2.1. Estimation of the Maximum Expectable Efficiency

For more than 5 years, the P3HT:PCBM blend has been dominating the organic-solar-cell research. Although the material blend is well known and investigated, there are still discussions on the practical efficiency one may expect from that system. Although the device physics of polymer:fullerene bulk heterojunctions has been the object of many recent review articles[7] and book chapters,[8] it is still important to set the efficiency expectations for that material system.

Consider a material, say P3HT, that absorbs photons with wavelengths smaller than 675 nm (a band-gap energy $E_g \approx 1.85$ eV). Assuming that in a P3HT:PCBM blend the polymer defines the optical gap of the composite, one can calculate the absorbed photon density as well as the power density by combining the absorption spectrum with the sun's spectrum. The typical spectrum of the light impinging on the surface of the Earth is given by the ASTM Standard G159,[9] and named Air Mass 1.5 (AM1.5). The so-called AM1.5G, the overall reference for solar-cell characterization,[10] cumulates an integrated power density of 1000 $W\,m^{-2}$ (100 $mW\,cm^{-2}$), and an integrated photon flux of $4.31 \times 10^{21}\ s^{-1}\,m^{-2}$, distributed over a large range of wavelengths (280–4000 nm). Under these assumptions, a P3HT:PCBM layer can absorb, at best, 27% of the available photons and 44.3% of the available power, while the *ultimate efficiency*, as defined by Shockley and Queisser,[11] predicts a value of 34.6% for a semiconductor with a band gap of 1.85 eV. This difference arises from the fact that each photon having an energy E_v larger than E_g produces only one electronic charge q, extracted at a maximum potential E_g.

The external quantum efficiency (EQE) of a device is defined by the ratio of the collected electrons to the incident photons. The

Gilles Dennler received his Engineering and Masters Degrees at the National Institute for Applied Sciences, Lyon, France, in 1999. He obtained a first Ph.D. in plasma physics at the University of Toulouse, France, and a second in Experimental Physics at Ecole Polytechnique of Montréal, Canada. In 2003, he moved to the Linz Institute for Organic Solar Cells (Austria), where he was appointed Assistant Professor. He joined Konarka in September 2006, where he is currently Director of European Research.

Markus Scharber received an Applied Physics B.Sc. degree from Napier University Edinburgh, Scotland, a Masters Degree from the Johannes Kepler University Linz, Austria, and a Ph.D. at the Linz Institute for Organic Solar Cells. He joined the company Quantum Solar Energy Linz (QSEL) in 2002, which was acquired by Konarka Technologies Inc. in 2003. Over the last 5 years, his main research activities have been new materials for efficient plastic solar cells and their efficiency limitations.

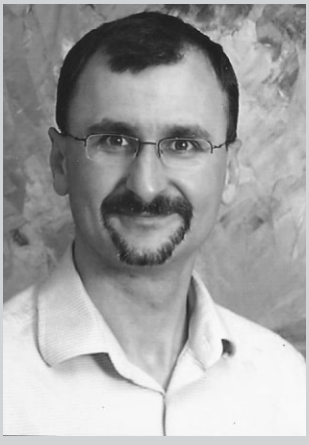

Christoph J. Brabec is the CTO of Konarka technologies Inc. He received his PhD in physical chemistry in 1995 from Linz university, joined the group of Prof Alan Heeger at UCSB for a sabbatical, and continued to work on organic semiconductors as assistant professor at Linz university with Prof. Serdar Sariciftci. He joined the SIEMENS research labs as project leader for organic optoelectronic devices in 2001 and finally joined Konarka in 2004.

short-circuit current density J_{sc} is expressed by:

$$J_{sc} = \frac{hc}{q} \int_{\lambda_1}^{\lambda_2} \frac{P_{AM1.5G}(\lambda) \cdot EQE(\lambda) \cdot d\lambda}{\lambda} \quad (1)$$

where h is Plank's constant, c is the speed of light in vacuum, and λ_1 and λ_2 are the limits of the active spectrum of the device. In the case of the P3HT:PCBM blend, and for an EQE of 100%, the maximum possible J_{sc} is about 18.7 mA cm^{-2}. If the average EQE is only 50%, J_{sc} would then be only about 9.35 mA cm^{-2}. More information about expected efficiencies and accuracy of measurement can be found in the literature.[10,12]

In a real device, the absorption in the photoactive blend cannot be 100%, because the active layer (AL) is embedded within a stack of several layers, which have different complex refractive indexes. Thus, absorption can occur in some layer located between the incident medium and the AL, and reflection can happen at any interface located before the bulk of the active layer. In order to precisely quantify the amount of light absorbed within the active layer, one needs first to calculate the 1D distribution of the optical electromagnetic field $E(x)$ across the device in any of the layers involved. This is usually solved by the so-called transfer-matrix formalism (TMF), which incorporates both the absorption and the reflection events in each subsequent layer.[13–15]

Figure 1 summarizes the number of photons (N_{ph}) absorbed in the P3HT:PCBM layer versus the thickness of this layer for an organic solar cell having the following structure: glass (1 mm)/ indium tin oxide (ITO, 140 nm)/poly(3,4-ethylenedioxythiophene): poly(styrenesulfonate) (PEDOT:PSS, 50 nm)/P3HT:PCBM (x nm)/ Al (100 nm). The refractive indexes used for this calculation can be found elsewhere.[16] It appears, in this figure, that N_{ph} generally increases with increasing thickness, but not monotonically. If the thickness of the layers is smaller than the coherence of the light, interference occurs, because the light is reflected by the opaque electrode. About 9.5×10^{16} photons s^{-1} cm^{-2} are absorbed in an AL of 5 μm. Assuming an average internal quantum efficiency (IQE) of 100%, this represents a J_{sc} value of 15.2 mA cm^{-2}, or approximately 20% less than in the theoretical consideration.

In the case of an AL that has a more realistic thickness of 400 nm, the maximum J_{sc} (IQE = 100%) is 12.8 mA cm^{-2}. If the average IQE is lower than 100%, J_{sc} is further reduced. At 80% average IQE, J_{sc} should be around 10.2 mA cm^{-2}. Thus, despite the fact that the theoretical short-current density of a

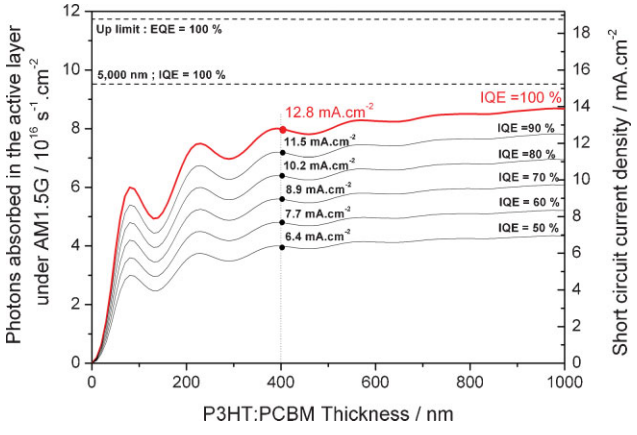

Figure 1. Number of photons (N_{ph}) absorbed in the active layer (AL) under AM1.5G calculated by TMF, for a device having the following structure: glass (1 mm)/ITO (140 nm)/PEDOT:PSS (50 nm)/P3HT:PCBM (x nm)/Al (100 nm). The right axis represents the corresponding short-circuit current density J_{sc} at various IQE, indicated in the graph.

Table 1. Nonexhaustive survey of reports focusing on photovoltaic devices based on P3HT:PCBM blends.

Year	P3HT Provider	M_w [g mol^{-1}]	Ratio to PCBM (weight)	Layer thickness [nm]	Solvent	Annealing time [min]	Annealing Temp. [°C]	Max EQE [%]	V_{oc} [V]	FF	J_{sc} [mA cm^{-2}]	Eff [%]	Light intensity [mW cm^{-2}]	Ref.
2002	–	–	1: 3	350	–	–	–	76	0.58	0.55	8.7	2.8	100	[24]
2003	–	–	–	110	DCB	4	75	70	0.55	0.6	8.5	3.5	80	[25]
2004	Rieke	–	1: 2	350	CB	4	75	65	0.54	0.37	15.2	3.1	100	[26]
2005	Rieke	100 000	1: 1	70	DCB	60	120	58	0.615	0.61	7.2	2.7	100	[27]
2005	Merck	11 600	1: 1	–	CB	15	140	58	0.61	0.53	9.4	3.0	100	[28]
2005	–	–	1: 1	63	DCB	10	110	–	0.61	0.62	10.6	4.0	100	[29]
2005	Rieke	–	1: 1	220	DCB	10	110	63	0.61	0.67	10.6	4.4	100	[30]
2005	Aldrich	87 000	1: 0.8	–	CB	5	155	–	0.65	0.54	11.1	4.9	80	[31]
2005	Rieke	–	1: 0.8	–	CB	30	150	–	0.63	0.68	9.5	5.0	80	[32]
2006	Merck	21 100	1: 1	175	CB	120	140	70	0.6	0.52	12	4.4	85	[33]
2006	–	–	1: 0.8	–	CB	10	150	88	0.61	0.66	11.1	5.0	90	[2]
2006	Rieke	–	1: 1	320	DCB	10	110	82	0.56	0.48	11.2	3.0	100	[34]
2008	Rieke	–	1: 1	220	DCB	10	120	87	0.64	0.69	11.3	5.0	100	[118]

P3HT:PCBM blend could be close to 19 mA cm^{-2}, the practically achievable J_{sc} of real devices will be in the range of 10–12 mA cm^{-2}.

2.2. Review of Experimental Results

The first years of OPVs were dominated by poly[2-methoxy,5-(2′-ethyl-hexyloxy)-*p*-phenylene vinylene) (MEH-PPV)/C_{60} composites, which were later on substituted by the better-processable combination of poly[2-methoxy-5-(3′,7′-dimethyloctyloxy)-1,4-phenylene vinylene] (MDMO-PPV)/1-(3-methoxycarbonyl) propyl-1-phenyl[6,6]C_{61} (PCBM).[1,17–21] Because of the rather large gap and low mobility of the PPV-type polymers, efficiencies remained at 3% at best,[22,23] and the general interest in this class of material faded.

During the last five years, research efforts have focused on poly(alkyl-thiophenes), and in particular on P3HT. In 2002, the first encouraging results for P3HT:PCBM solar cells with a weight ratio of 1:3 were published.[24] At that time, the short-circuit current density was the largest ever observed in an organic solar cell (8.7 mA cm^{-2}), and resulted from an EQE that showed a maximum of 76% at 550 nm. This paper appeared to be a starting point for a rapid development for the P3HT:PCBM blend, followed by the first explicit reports on efficiency enhancement in P3HT/PCBM cells as a result of thermal annealing.[25] The main development over the last years has consisted in understanding and optimizing the processing of the active layer and, especially, the device annealing conditions, which, until recently, appeared to be mandatory to achieve high efficiencies. Table 1 gives a nonexhaustive survey of reports that deal with efficient photovoltaic cells based on a P3HT:PCBM blend.[2,26–35]

Controlling the morphology of the bulk heterojunction in order to ensure maximum exciton dissociation at the interface between the donor and the acceptor, in parallel to an efficient charge-carrier extraction, was found to be the key for high performance. The optimum P3HT:PCBM weight ratio for that is about 1:1, and the two best-suited solvents for this blend are chlorobenzene (CB) and ortho-dichlorobenzene (oDCB). Upon annealing, the open-circuit voltage (V_{oc}) was usually found to decrease slightly, while both the J_{sc} and the fill factor (FF) increased significantly. Figure 2 illustrates a typical enhancement of the EQE upon thermal annealing, as reported by Yang et al.[27] This phenomenon is attributed mainly to an enhancement of the charge-carrier transport, by a larger hole mobility,[36,37] a reduced dispersivity,[38] and a reduced recombination kinetics.[39,40] X-Ray investigations allowed the development of a microscopic picture of the annealing process,[41] as depicted in Figure 3. Several detailed morphological studies revealed that the organization of the P3HT:PCBM is modified upon annealing,[27,32,36] with fibrillar-like P3HT crystals embedded in a matrix believed to comprise mostly PCBM nanocrystals and amorphous P3HT.[27]

The influence of the molecular weight (M_w) on the performance of P3HT:PCBM was quickly addressed once the annealing process was understood.[42] Too-short molecular-weight fractions were shown to have inferior mobility, most likely because of main-chain defects and low mobility.[43] Furthermore, the role of smaller M_w fractions was found to initiate or facilitate the growth of crystalline fibrils during the annealing step, leading to a large

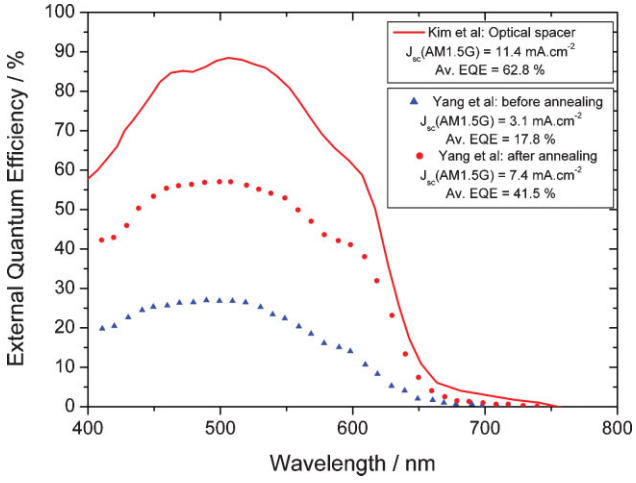

Figure 2. EQE of different P3HT:PCBM devices reported in the literature. Adapted from [27,2].

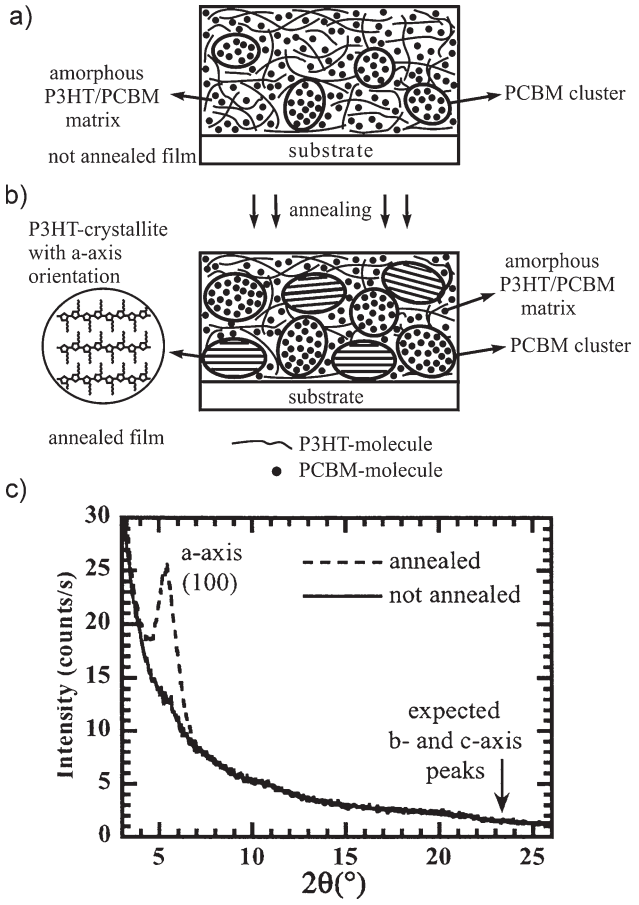

Figure 3. a,b) Schematic pictures showing the microscopic process during annealing. c) Grazing incidence X-ray spectrum on a blend before and after annealing, showing the evolution of the *a*-axis oriented P3HT crystals. Reproduced with permission from [41].

number of small crystals, while higher M_w P3HT stays amorphous.[43] On the other hand, too-high molecular weights produced highly entangled polymer networks, rendering annealing either impossible or requiring higher temperatures and/or longer annealing times.[44] The ideal morphology appears to be formed for P3HT with an average M_w in the range 30 000–70 000, and a rather high polydispersity of around 2, which gives a good mix of highly crystalline regions formed by low-M_w P3HT embedded in and interconnected by a high-M_w P3HT matrix.[45]

Like the effect of M_w, the influence of the polymer's regioregularity (RR) (defined as the percentage of monomers adopting a head-to-tail configuration, rather than a head-to-head) is critical. A specific threshold for RR (about 95%) seems to be necessary to give the highest J_{sc} and FF,[33] mainly because of the better transport properties of highly RR P3HT.[46]

2.3. Towards a Better Control of Morphology

As described above, P3HT:PCBM blends require thermal annealing in order to self-organize into a conformation that ensures optimum charge- carrier creation and extraction. But other ways of controlling the morphology have been proposed, and proven to be highly effective.

Slow drying was reported as one of the methods to improve the order in P3HT blends with PCBM.[30] The improved order[47] was reflected in a higher hole mobility,[48] higher FFs, and a reduced series resistance.

Additives were reported as an alternative method to create better order in blends of P3HT and PCBM. Oleic acids and alkylthiols of different lengths,[49] like n-hexylthiol, n-octylthiol, or n-dodecylthiol,[50] were added to P3HT/PCBM solutions, and allowed the formation of thin films with slightly enhanced hole mobility and significantly enhanced charge-carrier lifetimes, because of enlarged P3HT domains with higher crystallinity. Nevertheless, some thermal annealing was still necessary to give the highest possible performance.

This approach is actually very similar to a technique that employs miniemulsions, described earlier and in detail by others.[51,52] In that approach, a mixture of P3HT in water, surfactants, and a solvent was rigorously sonicated, before allowing the solvent evaporate. Such dispersions typically have a particle distribution between 70–200 nm, and give homogeneous films[53] upon spin coating. Field-effect-transistor mobilities for such nanoparticular films were found to be on the order of 10^{-4}–10^{-3} $cm^2 V^{-1} s^{-1}$. Solar-cell fabrication was more difficult, because there are no known well-performing, water-soluble fullerenes. Thus, only investigations of bilayer devices were performed, which exhibited moderate performances.[54]

A third, quite similar approach to control the nanomorphology of P3HT/PCBM blends requires the addition of 'nonsolvents' into the P3HT/PCBM solution (Fig. 4).[55,56] This phenomenon is attributed to the aggregation of the polymer into nanoparticulates, similar to the miniemulsion mentioned above. Addition of nitrobenzene (NtB) to a P3HT/PCBM solution in chlorobenzene allows an increase in the volume fraction of P3HT aggregates from some 60% to up to 100% with increasing NtB content. Photovoltaic devices from P3HT/PCBM mixtures with NtB as additive allowed the manufacture of devices with efficiencies as high as 4% without thermal annealing. These experiments proved that a good part of the thin-film morphology can already be introduced on the solution level.

Creating order in the P3HT phase is the key to high performance.[57] The most recent approach grew fibers[57,58] by slow cooling of P3HT solutions, with the crystalline fibers being isolated from the amorphous material by centrifugation and filtration. The fibers were reformulated in dispersions with PCBM, and used for solar-cell processing. The best results (efficiency up to 3.6% under 100 $mW cm^{-2}$) were obtained for a mixture of 75% P3HT fibers and 25% disorganized P3HT, the latter being suspected necessary to fill the gaps present in the nanostructure layer, and to ensure intimate contact between the donor fibers and the PCBM domains (Fig. 5).[57]

3. Alternative Promising Materials

The efficiency table number 31 published in the *Journal Progress in Photovoltaics*,[6] which summarises the recorded efficiencies of several solar-cell technologies, holds two entries related to organic

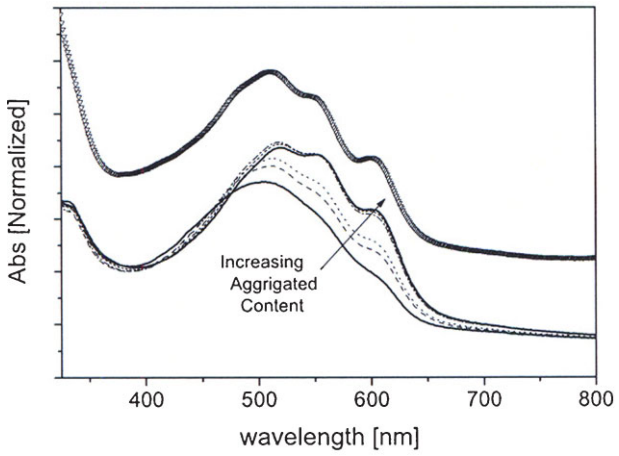

Figure 4. UV-vis spectra of 3:2 P3HT:PCBM as-cast PV devices with 0% (solid line), 0.33% (dashed line), 0.67% (dotted line), 1.6% (dashed–dotted line), 3.2% (short dashed line), and 6.3% (solid line) nitrobenzene added into the chlorobenzene solvent. Offset from the other spectra is the as-cast PV device from the *o*-xylene dispersion (triangles). Reproduced with permission from [56].

solar cells. In both cases, efficiencies of $>5\%$ are reported for bulk-heterojunction solar cells prepared from a blend of a conjugated polymer and a fullerene. The devices were characterized by the NREL (National Renewable Energy Laboratory, Boulder Colorado) calibration laboratory. The report lists the efficiency numbers, and includes the open-circuit voltage, the electrical fill factor, and the short-circuit current, but does not disclose a detailed description of the applied materials. However, analyzing the device parameters reveals that both solar cells are not composed of a blend of regioregular P3HT and PCBM, both deliver significantly higher open-circuit voltages ($V_{oc} > 850$ mV) compared with the best P3HT-PCBM solar cells (see Table 1), and either alternative donor or acceptor materials were applied to achieve these record efficiencies.

The efficiency limitations of organic solar cells have been described earlier,[59,60] discussing the importance of the band gap, that is, the highest occupied molecular orbital (HOMO) and lowest unoccupied molecular orbital (LUMO) levels of the donor and the acceptor molecules. Figure 6 shows a schematic drawing of the energy levels in an organic solar cell. The maximum short-circuit current is determined by the smaller optical band gap of the two materials, and V_{oc} is proportional to the difference between the HOMO level of the donor material and the LUMO level of the acceptor compound. For an efficient charge generation in the donor–acceptor blend, a certain offset of the HOMO and LUMO levels (ΔE_{HOMO}, ΔE_{LUMO}) is required,[61] which is believed to be a few hundred milli-electron Volts.

This offset, which is often referred to as the exciton binding energy,[62] determines the ultimate device efficiency of bulk-heterojunction solar cells.[59,60] For a minimum energy offset of 0.3 eV between the donor and acceptor, power conversion efficiencies of $>10\%$ are pratical,[60] for a semiconductor with an ideal optical band gap of $\sim$1.4 eV (Fig. 7), at an EQE of 65%, and a FF of 65%. The maximum efficiency does not depend on the absolute position of the HOMO and LUMO levels, but is solely a function of the smaller band gap and the donor–acceptor level offsets.

For donor band gaps smaller than $\sim$3 eV, Figure 7 describes the efficiency of bulk-heterojunction solar cells that comprise a donor with a variable band gap in conjunction with an acceptor with a variable LUMO. For highest efficiencies, the difference between the LUMO levels needs to be 0.3 eV, and a band gap in the range of 1.2–1.7 eV, which would correspond to donor HOMO levels of –5.2 to –5.7 eV if the acceptor is PCBM (whose LUMO is assumed to be -4.3 ev). The material-design rules described above suggest that optimising the LUMO-level difference is the most promising strategy to develop high-efficiency bulk-heterojunction solar cells.

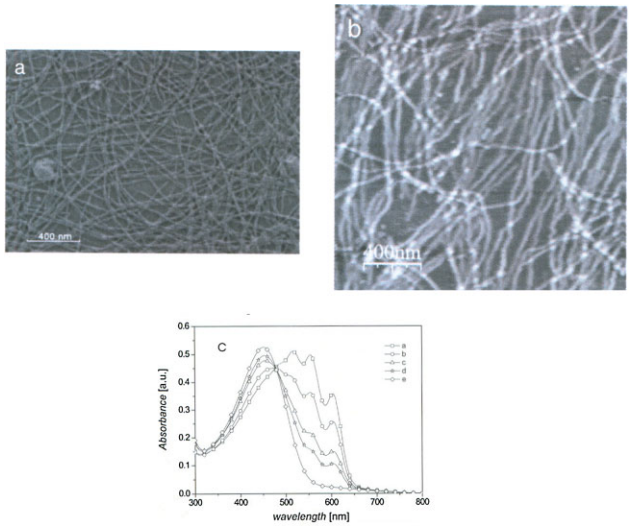

Figure 5. a) Scanning electron microscopy and b) atomic force microscopy images obtained for a 0.05 wt% P3HT solution in cyclohexanone. b) Absorption spectra of a 1 wt% P3HT solution in *p*-xylene, with different proportions of nanofibers and well-solubilized P3HT: a) 97%, b) 75%, c) 50%, d) 39%, and e) 0% nanofibers. Reproduced with permission from [56].

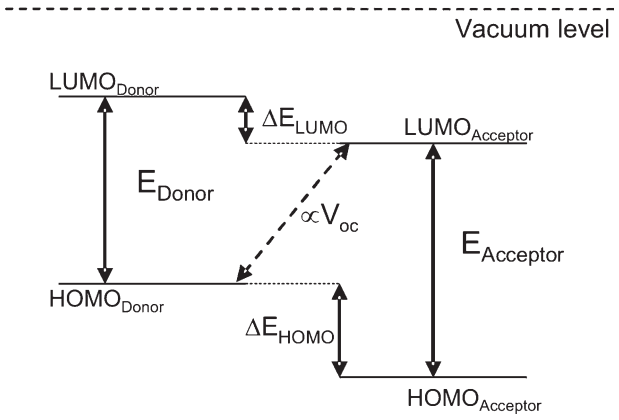

Figure 6. Schematic drawing of the donor and acceptor energy levels.

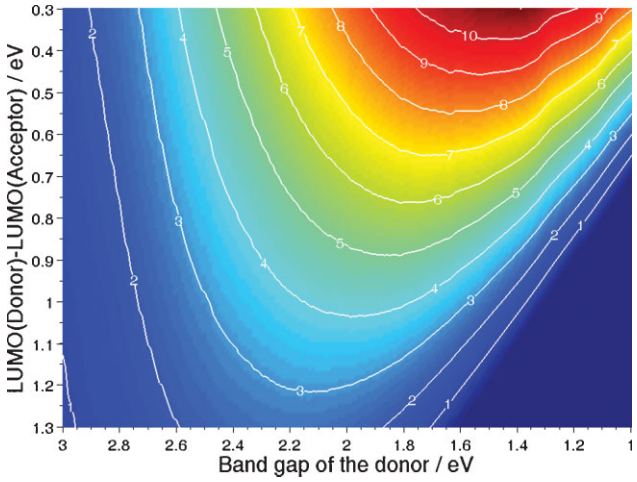

Figure 7. Calculated efficiency under AM1.5G illumination for single-junction devices based on composites that consist of a donor with a variable band gap and LUMO level and an acceptor with a variable LUMO level.

The chemistry of conjugated polymers offers powerful methods to tune the HOMO and LUMO levels, and to modify the band gap of the material. In the so-called donor–acceptor approach,[63,64] alternating electron-rich (donor D) and electron-poor (acceptor A) units are coupled together to form the polymer backbone. For such a $(–D–A–)_n$ polymer, a second resonance structure $(–D^+–A^–)_n$ gains importance with respect to the neutral structure, and increases the double-bond character of the single bonds in the polymer. This consequent reduction of the bond-length alternation effectively modifies the HOMO and LUMO levels and the band gap of the polymer. Several promising candidates have been synthesized, and a noncomprehensive selection of materials will be discussed in the next section. At this point, we would like to stress that a favourable arrangement of the HOMO and LUMO levels of the donor and acceptor materials is a prerequisite for a highly efficient solar cell. In addition, an optimised nanomorphology of the donor/acceptor composite, as well as a sufficient charge transport (charge carrier mobilities in range of 0.001 $cm^2 V^{-1} s^{-1}$), are necessary for high power-conversion efficiencies.

3.1. Promising Donor Materials

Figure 8 summarizes a selection of high-potential structures for high performance.[65–70] Most of the structures are from the material classes of thiophene, fluorene, carbazole, and cyclopentadithiophene based copolymers. In addition, one typical low-band-gap polymer and a metallated conjugated polymer are discussed. All compounds have been tested in bulk-heterojunction solar cells in combination with PCBM. These materials have an efficiency potential between 7 and 10%, and up to ~6% power-conversion efficiency have already been reported for a few of them.

3.1.1. Fluorene-based Copolymers

In the past years, several different polyfluorene copolymers have been prepared and tested in solar cells.[65,66,71–73] Andersson et al. prepared more than 10 different polyfluorene (PF) derivatives called APFO polymers. This class of polymers offers a sufficiently large variability in the position of the HOMO/LUMO levels, and polymers with a low band gap that show a photosensitivity down to 1 μm (polymer 2, Fig. 8) were demonstrated. The APFO family is a successful demonstration of the donor–acceptor approach, and illustrates the high potential of this material class for organic solar cells. The highest power-conversion efficiency of a polyfluorene-based solar cell was reported by the ECN (Energy Research Center of the Netherlands). Bulk-heterojunction solar cells based on a blend of polymer 1 (Fig. 8) and PCBM were reported with an efficiency of 4.2% (AM1.5 corrected for the spectral mismatch). The external and internal quantum efficiencies[65] of these devices was found to have maximum values close to 60% and 75%, respectively, although the good performance of this polymer is mainly attributed to the high V_{oc} of ~1 V, which

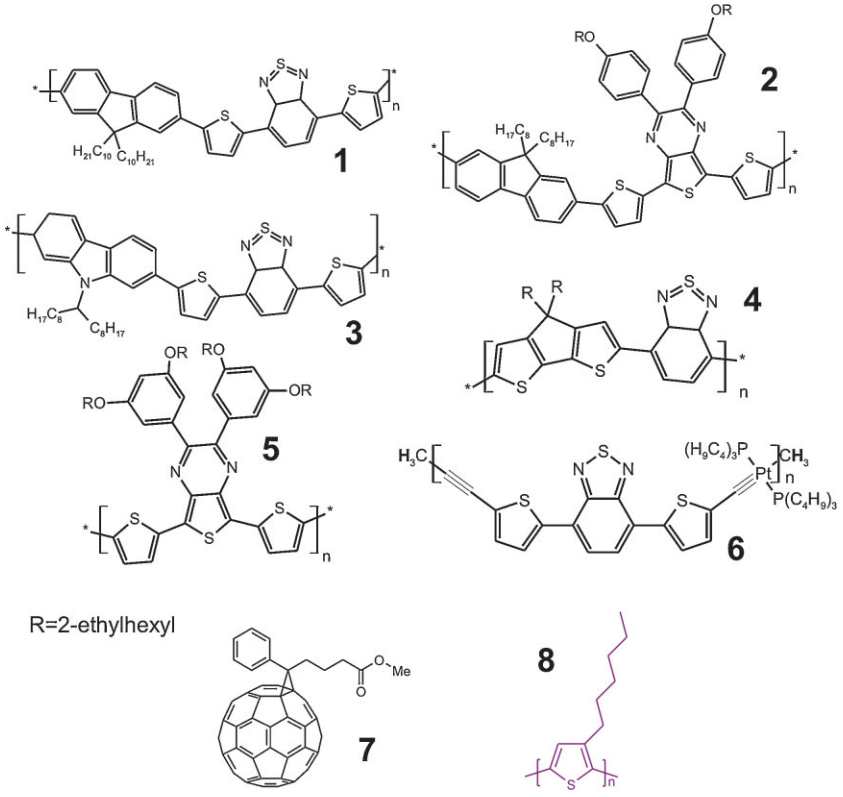

Figure 8. Promising polymers for OPV devices: 1) poly[9,9-didecanefluorene-alt-(bis-thienylene) benzothiadiazole] [65], 2) APFO-Green 5 [66], 3) poly[*N*-9′-heptadecanyl-2,7-carbazole-*alt*-5,5-(4′,7′di-2-thienyl-2′,1′,3′-benzothiadiazole)] [67], 4) poly[2,6-(4,4-bis-(2-ethylhexyl)-4*H*-cyclopenta[2,1-b;3,4-b2]-dithiophene)-*alt*-4,7-(2,1,3-benzothiadiazole)] [68], 5) poly{5,7-di-2-thienyl-2,3-bis(3,5-di(2-ethylhexyloxy)phenyl)thieno[3,4-b]pyrazine} [69], and 6) platinum(II) polyyne polymer [70]. 7) and 8) are PCBM and P3HT, repectively.

can compensate the rather low short-circuit current (7.7 mA cm^{-2}) and fill factor (54%). A high open-circuit voltage is a typical feature of fluorene-based polymer devices, as the polymers often have a low-lying HOMO level. An interesting variation of polymer 1 in Figure 8 is obtained by replacing the fluorene unit by dibenzosilole.[74,75] Replacing the bridging C atom of the fluorene by a Si atom is motivated by the expectation of a positive impact on the charge-transport properties. This idea is supported by the work of Wang et al.,[75] who reported an uncertified power-conversion efficiency of 5.4% for an alternating copolymer of 2,7-silafluorene and 4,7-di(2′-thienyl)-2,1,3-benzothiadiazole PCBM mixture.

3.1.2. Carbazole-based Copolymers

A few recent reports[67,76] have described the use of carbazole copolymers in solar cells. This material class appears to have identical electrical and optical properties to the polyfluorene class. Moulin et al. tested polymer 3 from Figure 8 in bulk-heterojunction solar cells with PCBM. The best device performance was in the range of 3.6% (measured at 90 mW cm^{-2}, 2, AM1.5, not certified or verified by EQE measurement), with a high V_{oc} of 890 mV and a high FF (63%). Overall, this specific polymer performed very similarly to the polyfluorene or polysilafluorene pendants (structure 1 in Fig. 8). Further work from the Leclerc group demonstrated the similarity between these material classes, and, by that, the high potential of 2,7-carbazole copolymers for solar-cell applications.[76]

3.1.3. Cyclopentadithiophene-based Copolymers

Cyclopentadithiophene-based polymers have attracted a lot of attention in the last two years,[3,68,77–79] with poly[2,6-(4,4-bis-(2-ethylhexyl)-4*H*-cyclopenta[2,1-*b*;3,4-*b*2]-dithiophene)-*alt*-4,7-(2,1,3-benzothiadiazole)] [PCPDTBT, structure 4, Fig. 8] as the most prominent candidate of this novel class of copolymers. This polymer is a true low-band-gap material ($E_g \sim 1.45$ eV), as well as an excellent charge transporter,[80] with high hole mobility, thereby fulfilling all the requirements for highly efficient solar cells. When PCBM is blended into PCPDTBT, an unfavourably intimate nanomorphology is formed, and the composites typically suffer from short carrier lifetimes and considerable recombination.[68] It takes the use of additives like alkanedithiols to form a more course nanomorphology. Heeger and coworkers[3] investigated the use and function of these additives in great detail, and reported solar cells with uncertified efficiencies beyond 5% for PCPDTBT/PCBM composites.

Konarka has explored the cyclopentadithiophene class in great detail, and, as one of the outcomes, Figure 9 shows an efficiency certificate for a device submitted to NREL. The solar cell delivers a short-circuit current of ~15 mA cm^{-2} and a V_{oc} of 575 mV, which results, together with an FF of 61%, in an efficiency of ~5.2%. The EQE of the certified device reaches ~63% at ~780 nm, with an estimated IQE of 85% at the same wavelength.

The only drawback of PCPDTBT is the rather high-lying HOMO level (~–5.2 eV), which does not allow open-circuit voltages higher than 600–700 mV when mixed with PCBM. The current research is, therefore, focused on two strategies to overcome this limitation. On the one hand, synthetic efforts are strengthened to design novel bridged bithiophene copolymers with lower-lying HOMO levels; on the other hand, novel acceptors with higher-lying LUMO levels are investigated.[81]

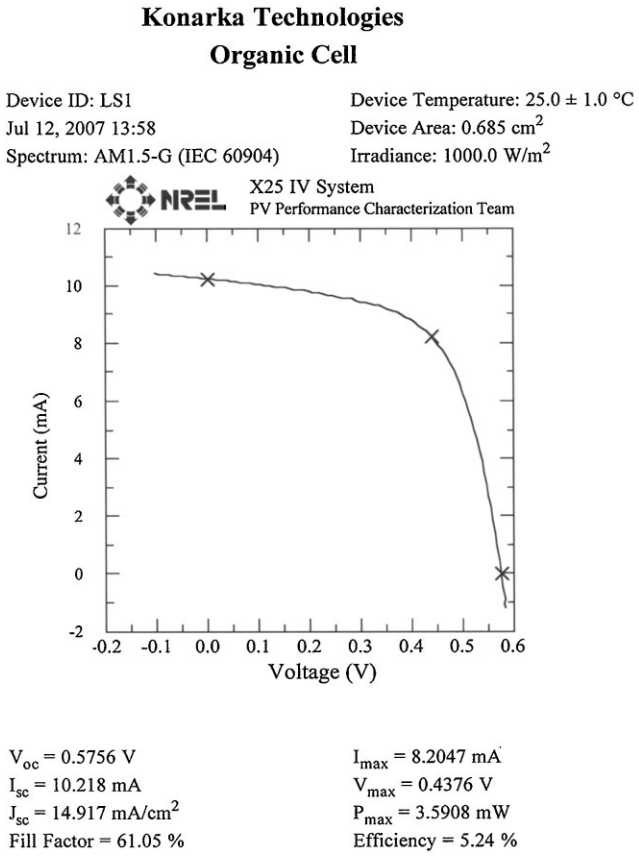

Figure 9. NREL certificate of the device LS1 submitted by Konarka.

3.1.4. Metallated Conjugated Polymers

Metallated conjugated polymers have attracted a lot of attention as emitter materials in polymer light-emitting diodes (PLED).[82–85] The metal atom integrated into the polymer backbone can increase the mixing of the first excited singlet and triplet states, leading to higher electroluminescence quantum efficiencies of PLEDs. In contrast, metallated conjugated polymers have rarely been tested as donor materials in bulk-heterojunction solar cells.[86,87] In early reports, power-conversion efficiencies significantly below 1% were published. Recently, Wong et al.[70] demonstrated highly efficient bulk-heterojunction solar cells using polymer 6 (Fig. 8) as a donor and PCBM as an acceptor material. The authors report ~5% power-conversion efficiency, with EQEs as high as 87% at 570 nm. Several groups raised serious doubts that the reported efficiencies were significantly overestimated,[88,89] and a verification by an independent institution is still missing today. Nevertheless, the concept to design polymers involving triplet states and long-lived triplet excitons in charge generation could become interesting for a next-generation organic PV material.

3.2. Promising Acceptor Materials

PCBM[19] was first reported in solar-cell applications in 1995,[1] and since then no significant better acceptor has been found. The ideal acceptor material for a bulk-heterojunction solar cell should have a strong absorption complementary to the absorption profile of the donor. Furthermore, the LUMO-level offset of the donor to the acceptor needs to be optimized, to ensure efficient charge transfer and a high open-circuit voltage at the same time. Finally, the acceptor needs to exhibit sufficient electron mobility in composites with the donor. Several acceptor molecules have been tested in bulk-heterojunction solar cells, among them conjugated polymers, fullerenes, carbon nanotubes, perylenes, and inorganic semiconducting nanoparticles.[90] So far, only derivatives of C_{60} and C_{70} have been reported to give highly efficient bulk-heterojunction devices, despite the fact that the position of the HOMO and LUMO levels and the optical absorption are not ideal for most of the donor polymers.[60]

A significant number of other C_{60} and C_{70} derivatives have been synthesized, to improve the processability, vary the HOMO/LUMO levels, or influence the morphology in blends with conjugated polymers.[91–93] Despite all these valuable efforts, it is the shift of the acceptor LUMO level that can give the biggest boost in efficiency. In the case of P3HT/PCBM blends, the acceptor level offset is ~1 eV. Thus, more than 50% of the available energy after photo-excitation is lost. A reduction of the LUMO offset would be directly translated in an increased open-circuit voltage (see Fig. 6). A novel acceptor with a ~600 mV higher-lying LUMO level, compared with PCBM, could theoretically double the efficiency of P3HT-based bulk-heterojunction solar cells. Up to now, only small shifts (< 100 meV) of the LUMO level of derivatized C_{60} have been achieved, by attaching electron-donating groups to the carbon cage.[91] At the time this review was written, Hummelen and coworkers reported and successfully demonstrated an exciting pathway to utilize fullerene multiadducts, which have 100–200 mV higher-lying LUMO values, compared to pristine C_{60}.[81]

4. Tandem Cells

As explained at the beginning of this review, the two major losses that occur in solar cells are the sub-band-gap transmission and the thermalization of the hot charge carriers.[94] One way to circumvent both effects simultaneously is the realization of tandem solar cells. Indeed, stacking-series-connected subcells have been shown to allow theoretical efficiency beyond the Shockley-Queisser limitation: While the maximum efficiency of a single cell under nonconcentrated sunlight is calculated to be about 30%, this value rises to 42% for a tandem that comprises two subcells with band gaps of 1.9 and 1.0 eV, respectively, and to 49% for a tandem that comprises three subcells with band gaps of 2.3, 1.4, and 0.8 eV, respectively.[95] Experimentally, efficiencies as high as 33.8%[96] have been recently measured on devices based on GaInP/GaInAs/GaInAs under nonconcentrated AM1.5G.

In the specific case of organic solar cells, the tandem approach allows researchers to tackle two additional limitations intrinsic to π-conjugated molecules. The first one is the poor charge transport, which hinders the realization of a thick active layer that would absorb maximum light. The second relates to the very nature of light absorption in those materials, which yield an absorption spectrum made of discrete broad peaks rather than a continuum. Hence, a combination of various different materials can help to more efficiently cover the emission spectrum of the sun. The series connection between the two devices is the critical technology for tandem cells. In many cases, thin (1–2 nm) metal layers are used as recombination layers. This recombination layer appears necessary to induce the alignment of the quasi-Fermi level of the acceptor of one cell with the donor of the second cell, as depicted in Figure 10. Other methods and materials for recombination layers will be discussed below.

The very first organic tandem cell published in the literature was realized with small molecules.[97] This report was followed by a series of publications that utilized various evaporated organic molecules.[15b,98–103] Small molecules are indeed very attractive for tandem cell manufacturing, since i) any interference of the individual layers as a result of solvent diffusion is absent and ii) the recombination layer is typically an evaporated metal layer a few nanometers thick.

Partially and fully solution-processed bulk-heterojunction tandem solar cells were realized significantly later than the small-molecule technology. The first reported devices consisted of a stack of two (poly[2-(3,7-dimethyloctyloxy)-5-methyloxy]-*para*-phenylene vinylene) (MDMO-PPV):1-(3-methoxycarbonyl)propyl-1-phenyl[6,6]C_{61} ($PC_{60}BM$) devices,[104] interconnected by a direct-current magnetron sputtered ITO layer. The first tandem cell comprising two different absorbers was realized by hybrid

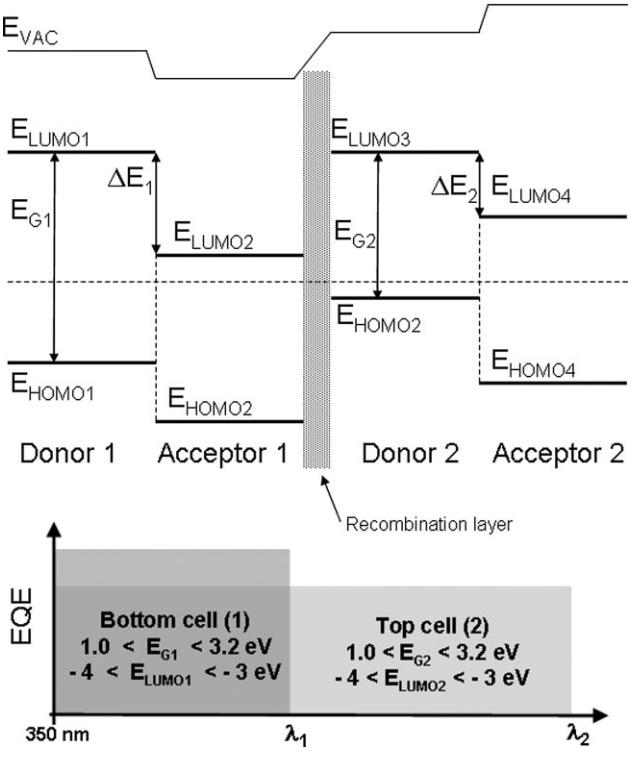

Figure 10. Simplified band diagram of tandem cells composed of two subcells connected in series by a recombination layer.

technology,[105] based on a bottom cell processed from solution (P3HT:PCBM) and a top cell evaporated (ZnP_C:C_{60}), both subdevices being separated by 1 nm of Au. Further reports followed up this hybrid solution, with other material combinations.[106]

In parallel, the first tandem cells that comprise two solution-processed subcells, based on a wide-band-gap polyfluorene-type polymer and a low-band-gap poly(terthiophene)-type polymer, were reported.[107] Dissolution of the first layer was prevented by using a composite middle electrode of 15 nm of evaporated metal, which is still semitransparent. The most significant innovation in the tandem technology reported the use of a solution-processed recombination layer, which, for the first time, allowed complete solution-processing of tandem cells.[108] This recombination layer was realized by spin-coating a ZnO nanoparticle[109] n-type layer as an electron selective electrode on the semiconductor, followed by an again spin-coated pH-neutralized PEDOT film as a hole-selective electrode for the top cell. The combination of a p-type and an n-type semiconductor layer created a barrier for Ohmic transport, enforcing recombination of electrons and holes at the interface with equal rates.

The highest-efficiency tandem devices reported to date are entirely solution processed. These devices had a 38% performance increase versus the best single device,[4] and an uncertified efficiency of 6.5% was reported (see Fig. 11). The intermediate layer comprised a TiO*x* sol–gel layer and a PEDOT:PSS layer; the bottom cell was made of a blend of PCPDTBT and PCBM, and the top cell was based on a P3HT:PC_{70}BM mixture. Noticeably, the selective usage of PC60BM or PC70BM allowed maximization of the number of photons absorbed in each subcell, because of a reduction of the overlap between the respective absorption spectrum of the active blends.[110]

Although all the devices reviewed above are based on a two-terminal concept comprising cells connected in series, several groups followed other approaches. The optimization of semi-transparent top electrodes allows the superposition of two independent devices, and connects them either in series or in parallel.[111] Monolithic four-terminal devices[112] were reported using a transparent and insulating polymer (polytrifluoroethylene) to separate the two stacked cells.[113] The most innovative device architecture, which is also accounted for under tandem cells, is probably the so-called folded reflective tandem device,[114] as depicted in Figure 12.

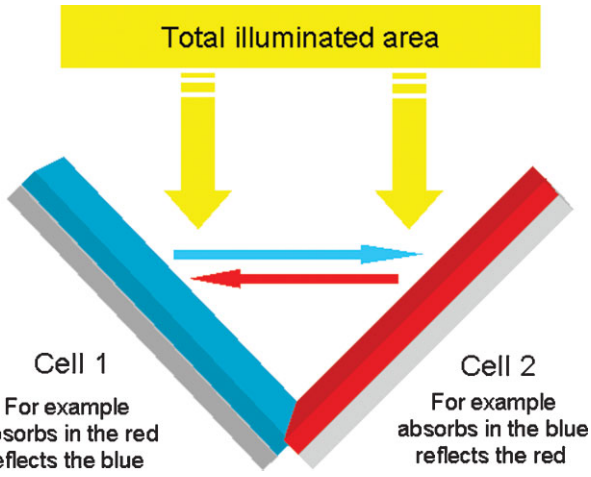

Figure 12. Sketch of the folded tandem cell realized by Tvingstedt et al. [114].

This geometry has three major advantages. First of all, the reflected light of one cell is directed toward the second device, which ideally has a complementary absorption spectrum. Second, the tilting of each cell enlarges the light path within the active layer.[115] Finally, using an angle between the cells smaller than 90° can cause a light-trapping effect to occur, significantly enhancing the absorption, and hence the photogeneration, of charge carriers. In the case of solar cells with thin active layers (50–60 nm) and rather low EQEs, an almost two-fold enhancement of the performance was reported for an angle of 40° between the cells. In the case of highly efficient single-junction cells, the V-shape geometry is only beneficial if semiconductors with two different band gaps are operated.

Table 2 gives an overview on the literature reports for organic tandem devices, and includes reports on small-molecular cells. Finally, and in analogy to the performance prediction for single-junction cells, Figure 13 predicts the efficiency for tandem cells in relation to the band gap of the single-junction materials. The prediction was calculated for the case of optimal aligned LUMO levels with only a 0.3 eV difference to the PCBM LUMO. The 2D contour lines show that the efficiency can reach values as high as 14%.[103]

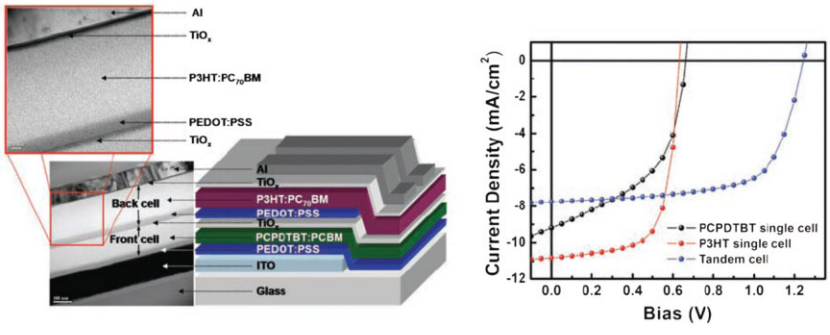

Figure 11. Structure and current-voltage characteristics of the tandem cells realized by Kim et al. Reproduced with permission from [4]. Copyright 2007 American Association for the Advancement of Science.

5. Fundamental Losses and Theoretical Efficiency of Organic Solar Cells

The fundamental question for any new solar technology is the determination of the ultimate efficiency. The analysis of the last two chapters predicted a technical feasible efficiency of over 10% for organic single-junction solar cells, and close to 15% for the tandem junction cells. Clearly, one could argue that the assumptions

Table 2. Nonexhaustive survey of reports dealing with stacked or tandem organic solar cells.

Year	Intermediate layer	Bottom cell					Top cell					Tandem cell				Ref.
		Active materials	V_{oc} [V]	FF	Jsc [mA cm^{-2}, (mW cm^{-2})]	Eff [%]	Active materials	V_{oc} [V]	FF	Jsc [mA cm^{-2}, (mW cm^{-2})]	Eff [%]	V_{oc} [V]	FF	Jsc [mA cm^{-2}, (mW cm^{-2})]	Eff [%]	
1990	2 nm Au	H2Pc/Me-PTC	0.44	–	2.7 (78)	–	as bottom	as bottom	as bottom	as bottom	as bottom	0.78	–	0.9 (78)	–	[97]
2002	0.5 nm Ag	CuPc/PTCBI	0.45	–	–	1.0	as bottom	as bottom	as bottom	as bottom	as bottom	0.9	0.43	6.5 (100)	2.6	[98]
2004	0.5 nm Ag	CuPc: C60	–	0.64	–	4.6	as bottom	as bottom	as bottom	as bottom	as bottom	1.03	0.59	9.7 (100)	5.7	[99]
2005	0.8 nm Au	ZnPc: C60	0.5	0.37	15.2 (130)	2.1	as bottom	as bottom	as bottom	as bottom	as bottom	0.99	0.47	10.8 (130)	3.8	[101]
2006	20 nm ITO + PEDOT:PSS	MDMO-PPV: PCBM	0.84	0.58	4.6 (100)	2.3	as bottom	as bottom	as bottom	as bottom	as bottom	1.34	0.56	4.1 (130)	3.1	[104]
2006	1 nm Au	P3HT: PCBM	0.55	0.55	8.5 (100)	2.6	ZnPc: C60	0.47	0.5	9.3 (100)	2.2	1.02	0.45	4.8 (100)	2.3	[105]
2006	0.5 nm LiF + 0.5 nm Al + 15 nm Au + 60 nm PEDOT:PSS	PFDTBT: PCBM	0.9	0.5	1.0 (100)	0.4	PTBEHT: PCBM	0.5	0.64	0.9 (100)	0.23	1.4	0.55	0.9 (100)	0.6	[107]
2007	30 nm ZnO + PEDOT	MDMO-PPV: PCBM	0.82	0.55	4.1 (100)	1.9	P3HT: PCBM	0.75	0.48	3.5 (100)	1.3	1.53	0.42	3.0 (100)	1.9	[108]
2007	8 nm TiOx + 25 nm PEDOT:PSS	PCPDTBT: PCBM	0.66	0.5	9.2 (100)	3.0	P3HT: PCBM	0.63	0.69	10.8 (100)	4.7	1.24	0.67	7.8 (100)	6.5	[4]

of the analysis, namely a rectangular EQE of 65% and a FF of 65%, can be overcome by careful device engineering and further reduction of bulk and interface recombination losses, which lead to higher efficiencies. But to answer the question of the ultimate efficiency of organic solar cells, a top-down approach appears more appropriate than a bottom-up approach, where the validity of technical assumptions dominates the result.

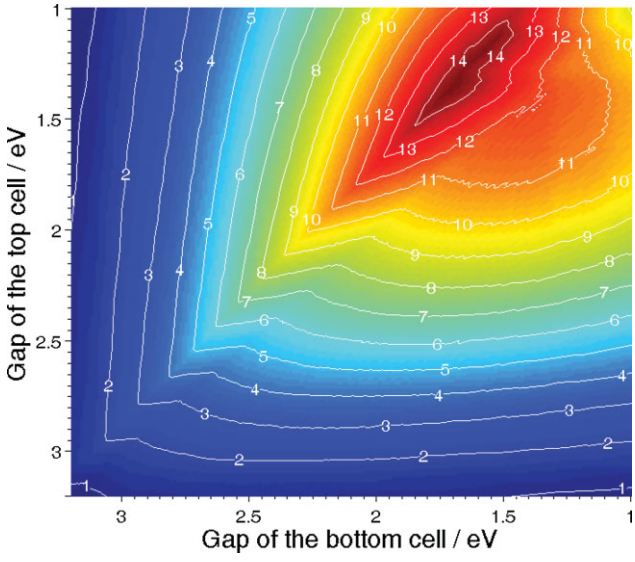

Figure 13. Efficiency of an OPV tandem device versus the band gap of both donors. We assumed that the difference between the LUMO of the donor and the acceptor is 0.3 eV, that the maximum EQE of the subdevices is 0.65, and that the IQE of the bottom device is 85% [103].

Shockley and Queisser[11] have used an elegant top-down approach to determine the maximum efficiency for single-junction solar cells, and their approach has been proven to be widely material and system independent. In contrast to their approach, we now introduce a calculation with a similarly generic but simpler photon balance, and then highlight three properties of organic solar cells that require the introduction of a specific loss analysis. These properties, described below, render organic bulk-heterojunction solar cells different from inorganic solar cells. i) The charge-carrier generation, that is, the photoinduced electron transfer, requires energy. ii) The charge carriers in organic solar cells are polarons that reside at energies different to the electric bands. The polaron energy, that is, polaron bands (single occupied molecular orbital (SOMO)), resemble the quasi-Fermi levels, and determine the maximum possible open-circuit voltage.[116] One should note that this situation is similar to the inorganics, where the quasi-Fermi level is always inside the bandgap. iii) The photocurrent of bulk-heterojunction solar cells has a strong electrical-field-dependent component, while organic semiconductors generally have low mobility.

The losses related to these properties are i and ii) reduction in the maximum possible open-circuit voltage and iii) reduction in the maximum possible FF.

To begin with, we summarize the assumptions used for the modeling:

- All photons resonant to the bandgap will be absorbed and contribute to the photocurrent.
- Photocurrent calculations are based on folding the absorption spectrum of the semiconductor with the AM 1.5G solar spectrum at an integrated intensity of 1000 W m^{-2}.[9] Although

early PV-cell efficiency calculations were based on a black-body spectrum, the AM1.5G spectrum has gained acceptance as the best representation of the sun's spectrum at the earth's surface.
- Possible dark current effects are neglected.
- The FF will be taken as a fixed value, instead of as a function of the band gap.

As introduced by Shockley, we will consider only a thermalized carrier. Excess energy, that is, the photon energy larger than the semicondcutor band gap, will be dissipated as heat.

Thermal radiation from the environment as well as thermal radiation from the solar cell itself will be neglected.

The balance of i) the photoinduced charge-transfer loss and ii) the polaron loss are material-related phenomena. Assuming i) thermalized-carrier loss equals the difference in the LUMO energies of the donor and the acceptor. Following Marcus theory, the rate of electron transfer in polarizable media is related to the driving force ΔG_0 (energy difference between the initial and the transferred state), which is related to the difference in the HOMO and LUMO energies. Although functional bulk-heterojunction composites with LUMO differences as low as 0.1 eV were reported,[117] we will use a value of 0.25 eV in the simulation. For the ii) polaron loss we will again assume a value of 0.25 eV.[116] It is important to note that these loss values are 'educated' assumptions, which allow one to discuss the impact of these fundamental loss mechanisms on performance. These losses will vary for the individual composites, and ii) specifically loss may deviate from the assumption for individual material systems.

Figure 14 shows efficiency versus band gap calculations for the various loss mechanisms. The local minima and maxima in the curves reflect the spectroscopic shape of the AM1.5G spectrum. The maximum efficiency of ~50% at ~1100 nm for a single-junction photovoltaic converter is reduced to approx. 40% at < 1000 nm (extrapolated), in the case of the charge-transfer loss (i), and to approximately 30% at 900 nm, in the case of combining the charge-transfer (i) with the polaron (ii) losses. Introduction of the two loss mechanisms shifts the optimum band gap to larger values, from 1100 nm (1.12 eV) down to 900 nm (1.37 eV).

To obtain more realistic benchmark values, we repeat the calculations for reasonable though challenging EQE and FF values. The highest EQE value reported for an organic solar cell is 87%.[118] FFs of > 70% have already been reported a few times. Note that the assumption of a fixed FF is a major difference compared with the Shockley model,[10] where the maximum power point is calculated as a function of the band gap, and reaches values between 0.8 and 0.9. As a compromise, an EQE of 90% and a FF of 70% were used to calculate the highest possible efficiency (Fig. 15). The reduction in FF and EQE do not change the spectroscopic shape of the efficiency versus band gap correlation. For each loss mechanism, the optimum band gap remains at the same position, but the absolute efficiency numbers are reduced. Even in the most unfavorable case, including all V_{oc}, EQE, and FF losses, an efficiency of a little less than 20% is realistic.

Inorganic and organic solar cells follow similar recombination mechanisms. Both their short-circuit current and FF are determined by the spectroscopic absorption, mobility, carrier lifetime, and defect distribution. The relation between radiative and nonradiative recombination may shift depending on the practical values, with the theoretical maximum remaining the same. As such, the Shockley–Queisser model would predict identical performance for inorganic and organic solar cells. The main difference, which is not accounted for in the Shockley–Queisser model, is the specific energetic loss (i), which leads to a reduction of the maximum-possible open-circuit voltage. The question arises as to whether we need to include the radiative recombination losses, which Shockley balanced under the dark current, for the organic-solar-cell prediction as well. The answer to this question is yes. Practically, we have accounted for these

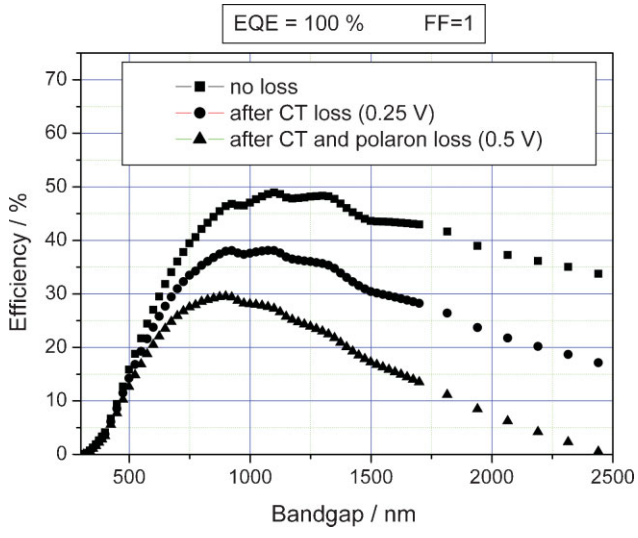

Figure 14. Plot of the theoretical maximum efficiency versus band gap for organic bulk-heterojunction solar cells: loss free case (full squares), including loss (i) (full circles) and including losses (i) and (ii) (full triangles). Both FF and EQE were set to 100% for this calculation.

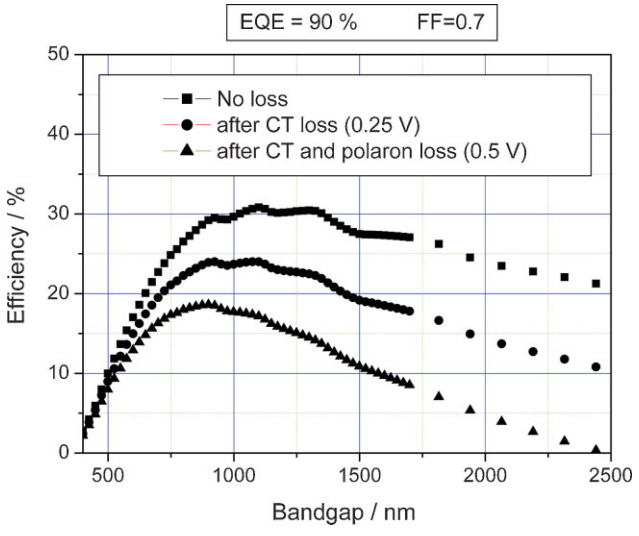

Figure 15. Plot of the practical maximum efficiency versus band gap for organic bulk-heterojunction solar cells: loss free case (full squares), including loss (i) (full circles) and including loss (i) and (ii) (full triangles). A FF of 70% and an EQE of 90% were used for this calculation.

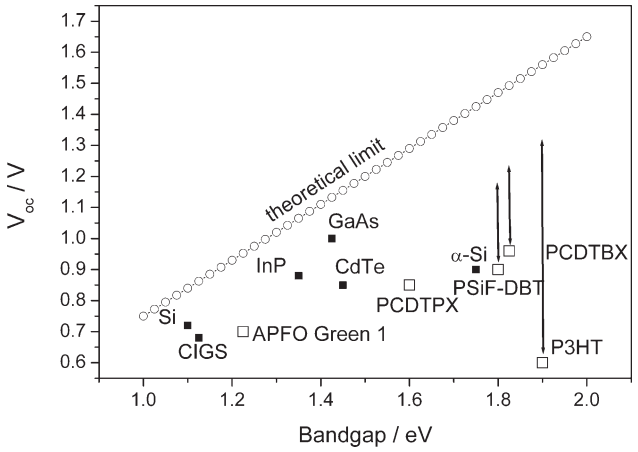

Figure 16. Plot of the V_{oc} for a few inorganic and organic semiconductors. The values for the inorganic semiconductors were taken from [119]. V_{oc} values for the organic semiconductors were taken from the following publications: PCDTQX and PCDTBX [76], APFO Green-1 [117], and PSiF-DBT [75]. The arrow indicates the potential for higher V_{oc} in case of a better-matched acceptor.

losses by introducing a respectably large value for the polaron losses.

A V_{oc} loss of the order of 0.25 V, as assumed due to the charge-transfer loss, would cause a significant disadvantage versus the inorganic technologies. It is important, therefore, to take a closer look and compare the V_{oc}-bandgap relation of organic semiconductors versus inorganic ones. Figure 16 summarizes typical V_{oc} values for the most popular inorganic semiconductors, among them Si, GaAs, copper indium gallium diselenide (CIGS), CdTe, and α-Si, together with a few selected values for organic polymers in bulk-heterojunction composites with PCBM. PCBM is not the ideal acceptor for some of the polymers listed, and arrows indicate V_{oc} values one may expect in the case of use of an optimized acceptor, that is, minimizing the LUMO differences between the acceptor and the donor to 0.25 eV. Interestingly, there are already a few wide-band-gap organic semiconductors with a E_g/V_{oc} ratios as favorable as for α-Si. For smaller band gaps, the organics clearly show a more unfavorable ratio compared with the best inorganics, like Si or GaAs.

In summary, a better understanding of the V_{oc} losses for organic solar cells is extremely important for more precise efficiency predictions and needs the highest attention in the next couple of years. A maximum practical efficiency of a little less than 30% is calculated for a polymer with a band gap of $\sim$ 1.4 eV in the absence of losses, while this maximum practical efficiency is reduced to approximately 20% in the case of losses. These calculations assumed the charge transfer and the polaron energy as the main losses.

6. The Economical Aspect—Can Lowest Costs Compensate for Lower Efficiency and Shorter Lifetime?

Organic PVs are marketed as a true-low-cost technology, and expectations are to meet costs of significantly less than 1 € per W_p in the full-production stage. On the other hand, there is general acceptance these PVs are unlikely to show superior performance and lifetime to Si or GaAs. It is, therefore, important to understand the minimum efficiency and lifetime a low-cost technology like OPV needs for market competitiveness; not only for niche markets, but also for mainstream PVs. That question needs to be answered in cents per kilowatt hour, and a cost model is required to calculate this number for an organic PV installation.

Costs in the photovoltaics business are typically separated into the costs for the module and the costs for the installation. The balance for the module costs is frequently called BOM (balance of modules). The balance of the installation costs is called BOS (balance of system). The BOM typically contains:

- All *material* costs, including material waste and process materials.
- All *production* costs, including capex, depreciation of machinery, maintenance, as well as the production yield.
- All *overhead* costs, including Research & Development, marketing, sales, etc.

The material costs for OPV will significantly change over time and with produced volume. However, a generic look to the BOM cost situation of OPVs today is already quite helpful at this early stage, and allows an educated guess of the upper and lower boundaries for the material costs. An informative cost analysis[120] of the single components required for OPV production gave a cost potential of 25 € m^{-2} and up to 100 € m^{-2}, whereas the 30–60 € m^{-2} regime appears as a reasonable cost scenario at fairly low production volumes.

The BOS typically contains:

- All *area-related* costs, including rent, mounting hardware, racks, shipping, installation, etc.
- All *energy-related* costs, including cables, converters, shipping, installation, servicing, etc.

A more precise summary of BOS and BOM costs for thin-film PVs can be found in the literature for the inorganic[121] as well as for the organic technologies.[120] Depending on the application (e.g., power PV, residential roof top, or commercial flat roof) and on the volume, BOS costs between some 100 € and 30 € were found to be reasonable for energy-cost calculations.

The focus of that analysis targets the development of an understanding to which extent a shorter product lifetime can be compensated for by significantly lower costs. As a model scenario, we will calculate the costs for a roof-top, residential PV installation.

The following assumptions are made:

- The installation is designed for a 1 MW annual capacity (equivalent to a 1 kW peak installation).
- The lifetime for the installation is 25 years.
- The module lifetime is varied between 3 and 10 years, and modules can be exchanged to complete the 25-year life cycle. A cost calculation for a 25-year lifetime installation can take a shorter-lifetime module into account, by a further investment at a later time. A module with 5 years of lifetime needs to be replaced four times within the 25-year life cycle. Replacement entails costs for the new modules plus an installation fee.
- The BOS costs are set to 70 € m^{-2}.

Table 3. Cost calculations in € per W_p for the presented model of 1 kW_p grid-connected roof-top plant under the following assumption: BOM = 50 € m^{-2} and BOS 70 € m^{-2}.

€ per W_p	3 years	4 years	5 years	6 years	7 years	8 years	9 years	10 years
3%	12.2	9.2	7.3	6.1	5.2	4.6	4.1	3.7
4%	10.4	7.8	6.3	5.2	4.5	3.9	3.5	3.1
5%	8.7	6.6	5.2	4.4	3.7	3.3	2.9	2.6
6%	8.2	6.1	4.9	4.1	3.5	3.1	2.7	2.5
7%	7.4	5.5	4.4	3.7	3.2	2.8	2.5	2.2
8%	7.1	5.3	4.3	3.5	3.0	2.7	2.4	2.1
9%	6.5	4.8	3.9	3.2	2.8	2.4	2.2	1.9
10%	6.3	4.7	3.8	3.1	2.7	2.4	2.1	1.9

- The BOM costs are varied between 10 to 100 € m^{-2} costs.
- The module efficiency is varied between 3 and 10%.

Discounting future investments: all future replacements and investment costs necessary to replace the shorter-lifetime PV modules are discounted by 7% to come with the net present value.

The last point is a major assumption on how to finance roof-top PVs. Debit financing, where a customer needs to take credit, is one way to finance an installation. In that case, the credit interest rates need to be added to the total costs for the installation.

Alternatively, the installation can be financed from an upfront investment. Less upfront investment is required for a module technology with shorter lifetimes, which allows discount of the future investments. We have chosen to work with the discount model, since it is clearly the more attractive model for a solar technology with a shorter lifetime. Nevertheless, it is important to note that the cost difference between these two models can be up to a factor of two.

Table 3 shows the first results from the calculations. The € per W_p costs of a 1 kW_p plant with a BOM of 50 € m^{-2} and a BOS of 70 € m^{-2} are summarized. Taking 3 € per W_p as a benchmark, a low-cost technology like OPV can become competitive at an efficiency of around 7% and a lifetime of 7 years.

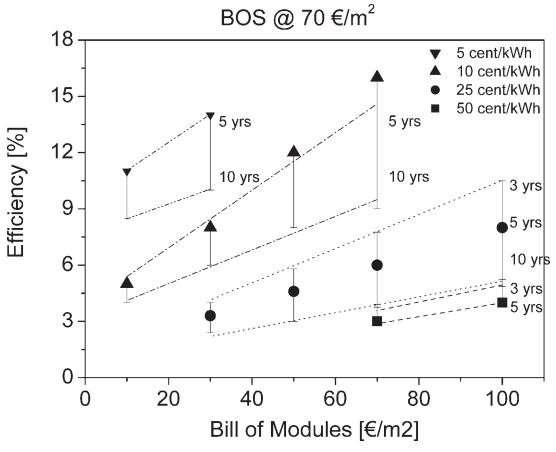

Figure 17. Energy-cost calculations in € cents kWh^{-1} for the presented model of 1 kWp grid-connected roof-top plant under the following set of assumptions: BOS 70 € m^{-2}; BOM: varied from 10–100 € m^{-2}; lifetime: varied from 3–10 years, efficiency: varied from 3–10%. The full symbols indicates the value at 5 years of lifetime. The error bars and the guided lines around the symbols show the parameter variation in the case of a 3 year and 10 year product, respectively.

It is by far more interesting and relevant to answer the question as to whether a low-cost and lower-performance technology, such as OPV, can be a sustainable solution for the supply of future energy. For this question, one has to calculate the costs of electricity in € cents per kilowatt hour. In our calculation, we assumed 1000 h of sun a year, a value typical for regions such as middle Europe (e.g., Germany). Figure 17 shows the costs in the case of 70 € m^{-2} BOS, whereas the performance parameters were varied to meet energy production costs of 50, 25, 10, and 5 cents kWh^{-1}, respectively. Additional calculations[120] for other BOS assumptions showed how great the BOS impacts the energy costs for a low-cost technology. Another clear relation is seen by the trend lines that connect the efficiency error bars. An increase in lifetime flattens out the dependence between costs and efficiency. Modules with a longer lifetime are much less susceptible to cost reduction upon efficiency increase (in absolute numbers). The calculations further show that it really pays off to have low module costs. The lower the module costs, the less important lifetime and efficiency become. At a BOM of 70 € m^{-2}, energy costs of 10 cents kWh^{-1} can be generated with module efficiencies between 8 and 16% for life times between 5 and 10 years. A module with 30 € m^{-2} costs can do the same with efficiencies between 5 and 8%. Better solar insulation is always favourable, independent of the costs. Running the calculation for 2000 h of sun per year would predict the same cost and lifetime values at only half of the efficiency.

The outcome of the cost calculation strongly supports the idea of low-cost and lower-performance PV technologies such as OPV. A shorter lifetime and lower efficiency can be compensated for by lower module costs. Low cost modules (i.e., a BOM of 30–50 € m^{-2}) with a lifetime between 5 and 10 years and an efficiency between 10 and 5% can produce electricity at 10 € cents kWh^{-1} in middle Europe, even at a BOS of 70 € m^{-2}.

7. Summary

Although P3HT is still dominating organic photovoltaic publication records, there are already several very promising alternative polymers available, which have led to certified efficiencies beyond the best values reported for P3HT. Polymers with various band gaps produced certified efficiencies of >5%. Novel material classes that are optimised for photovoltaic requirements will

rapidly lead to efficiencies beyond 7%, and their combination in multi-junction devices will lead to even higher efficiencies. Further improvement in the power-conversion efficiency of organic solar cells will come from donor–acceptor pairs with an optimised LUMO-level offset, as was demonstrated, for instance, by using multi-adduct fullerenes instead of single substituted fullerenes. Overall, 10% efficient organic solar cells appear to be within reach in the next few years.

The energy offset between the donor and acceptor LUMO levels required for an efficient electron transfer is a unique loss mechanism among photovoltaic technologies. This loss mechanism reduces the maximum achievable efficiency for the organic and hybrid bulk heterojunction technologies, and practical 'maximum' efficiencies between 20–25% appear reasonable.

Cost efficient power generation is achievable with low-cost solar-cell technologies, which show efficiencies at least between 5 and 10% and lifetimes between 5 and 10 years. These values depend on the precise module and installation costs. Cost-model calculations prove that the lower efficiency and lower lifetime of organic solar cells as compared with inorganic technologies can be compensated by their low-cost structure.

Received: May 10, 2008
Revised: July 23, 2008
Published online: February 9, 2009

[1] G. Yu, J. Gao, J. C. Hummelen, F. Wudl, A. J. Heeger, *Science* **1995**, *270*, 1789.
[2] J. Y. Kim, S. H. Kim, H.-Ho. Lee, K. Lee, W. Ma, X. Gong, A. J. Heeger, *Adv. Mater.* **2006**, *18*, 572.
[3] J. Peet, J. Y. Kim, N. E. Coates, W. L. Ma, D. Moses, A. J. Heeger, G. C. Bazan, *Nat. Mater.* **2007**, *6*, 497.
[4] J. Y. Kim, K. Lee, N. E. Coates, D. Moses, T.-Q. Nguyen, M. Dante, A. J. Heeger, *Science* **2007**, *317*, 222.
[5] R. Gaudiana, C. J. Brabec, *Nat. Photon.* **2008**, *2*, 287.
[6] M. A. Green, K. Emery, Y. Hishikawa, W. Warta, *Prog. Photovolt. Res. Appl.* **2008**, *16*, 61.
[7] P. W. Blom, V. D. Mihailetchi, L. J. A. Koster, D. E. Markov, *Adv. Mater.* **2007**, *19*, 1551.
[8] a) G. Dennler, N. S. Sariciftci, C. J. Brabec, in *Semiconducting Polymers*, 2nd ed. (Eds: G, Hadziioannou, G. G. Malliaras), Wiley-VCH, Weinheim **2006**, pp. 455–530.[b)]*Organic Photovoltaics: Materials, Device Physics, and Manufacturing Technologies* (Eds: C. J, Brabec, U, Scherf, V. Dyakonov), Wiley-VCH, Weinheim **2008**.
[9] American Society for Testing and Materials (ASTM) Standard G159, West Conshoken, PA, USA. Source: http://rredc.nrel.gov/solar/spectra/am1.5/.
[10] a) K. Emery, C. Osterwald, in *Current Topics in Photovoltaics*, Vol. *3*(Eds: T. Coutts, J. Meakin,), Academic, London, UK **1988**, Ch.4. b) V. Shrotriya, G. Li, Y. Yao, T. Moriarty, K. Emery, Y. Yang, *Adv. Funct. Mater.* **2006**, *16*, 2016.
[11] W Shockley,, H. J. Queisser, *J. Appl. Phys.* **1961**, *32*, 510.
[12] G. Dennler, T. Ameri, P. Denk, H.-J. Egelhaaf, K. Forberich, M. Koppe, M. Morana, M. C. Scharber, C. Waldauf, B. de Boer, K. Emery, G. Rumbles, J. M. Kroon, G. G. Malliaras, M. D. McGehee, J. Nelson, M. Niggemann, M. Pfeiffer, M. K. Riede, S. E. Shaheen, M. Wienk, *Materials Today* **2007**, *November*, 56.
[13] a) Z. Knittl, *Optics of Thin Films*, Wiley, London, UK **1976**. b) H. A. Macleod, *Thin film Optical Filters*, London Adam Hilger, London, UK **1986**. c) R. M. A. Azzam, N. M. Bashara, in *Ellipsometry and Polarized Light*, North-Holland, New York, USA **1977**.
[14] L. S. Roman, W. Mammo, L. A. A. Pettersson, M. R. Andersson, O. Inganäs, *Adv. Mater.* **1998**, *10*, 774.
[15] a) L. A. A. Pettersson, L. S. Roman, O. Inganäs, *J. Appl. Phys.* **1999**, *86*, 487. b) P. Peumans, A. Yakimov, S. R. Forrest, *J. Appl. Phys.* **2003**, *93*, 3693. c) H. Hoppe, N. Arnold, D. Meissner, N. S. Sariciftci, *Thin Solid Films* **2004**, *451*, 589.
[16] G. Dennler, K. Forberich, M. C. Scharber, C. J. Brabec, I. Tomic, K. Hingerl, T. Fromherz, *J. Appl. Phys.* **2007**, *102*, 054 516.
[17] a) Y. Wang, *Nature* **1992**, *356*, 585. b) S. Morita, A. A. Zakhidov, K. Yoshino, *Solid State Commun.* **1992**, *82*, 249. c) N. S. Sariciftci, L. Smilowitz, A. J. Heeger, F. Wudl, *Science* **1992**, *258*, 1474.
[18] N. S. Sariciftci, D. Baun, C. Zhang, V. I. Srdanov, A. J. Heeger, G. Stucky, F. Wudl, *Appl. Phys. Lett.* **1993**, *62*, 585.
[19] J. C. Hummelen, B. W. Knight, F. LePeq, F. Wudl, J. Yao, C. L. Wilkins, *J. Org. Chem.* **1995**, *60*, 532.
[20] V. D. Mihailetchi, J. K. J. van Duren, P. W. M. Blom, J. C. Hummelen, R. A. J. Janssen, J. M. Kroon, M. T. Rispens, W. J. H. Verhees, M. M. Wienk, *Adv. Funct. Mater.* **2003**, *13*, 43.
[21] S. E. Shaheen, C. J. Brabec, N. S. Sariciftci, F. Padinger, T. Fromherz, J. C. Hummelen, *Appl. Phys. Lett.* **2001**, *78*, 841.
[22] C. J. Brabec, S. E. Shaheen, C. Winder, N. S. Sariciftci, P. Denk, *Appl. Phys. Lett.* **2002**, *80*, 1288.
[23] a) P. W. M. Blom, M. J. M. De Jong, S. Breedijk, *App. Phys. Lett.* **1997**, *71*, 930. b) C. Melzer, E. J. Koop, V. D. Mihailetchi, P. W. M. Blom, *Adv. Funct. Mater.* **2004**, *14*, 865. c) V. D. Mihailetchi, L. J. A. Koster, P. W. M. Blom, C. Merzer, B. De Boer, J. K. J. van Duren, R. A. J. Janssen, *Adv. Funct. Mater.* **2005**, *15*, 795.
[24] P. Schilinsky, C. Waldauf, C. J. Brabec, *Appl. Phys. Lett.* **2002**, *81*, 3885.
[25] F. Padinger, R. S. Rittberger, N. S. Sariciftci, *Adv. Funct. Mater.* **2003**, *13*, 85.
[26] M. Riedel, V. Dyakonov, *Phys. Status Solidi A* **2004**, *201*, 1332.
[27] X. Yang, J. Loos, S. C. Veenstra, W. J. H. Verhees, M. M. Wienk, J. M. Kroon, M. A. J. Michels, R. A. J. Janssen, *Nano Lett.* **2005**, *5*, 579.
[28] Y. Kim, S. A. Choulis, J. Nelson, D. D. C. Bradley, S. Cook, J. R. Durrant, *Appl. Phys. Lett.* **2005**, *86*, 063502.
[29] G. Li, V. Shrotriya, Y. Yao, Y. Yang, *J. Appl. Phys.* **2005**, *94*, 043704.
[30] G. Li, V. Shrotriya, J. Huang, T. Mariarty, K. Emery, Y. Yang, *Nat. Mater.* **2005**, *4*, 864.
[31] M. Reyes-Reyes, K. Kim, D. L. Carroll, *Appl. Phys. Lett.* **2005**, *87*, 083506.
[32] W. Ma, C. Yang, X. Gong, K. Lee, A. J. Heeger, *Adv. Funct. Mater.* **2005**, *15*, 1617.
[33] Y. Kim, S. Cook, S. M. Tuladhar, S. A. Choulis, J. Nelson, J. R. Durrant, D. D. C. Bradley, M. Giles, I. McCulloch, C.-S. Ha, M. Ree, *Nat. Mater.* **2006**, *5*, 197.
[34] M. S. White, D. C. Olson, S. E. Shaheen, N. Kopidakis, D. S. Ginley, *Appl. Phys. Lett.* **2006**, *89*, 143517.
[35] H. Hoppe, N. S. Sariciftci, *J. Mater. Chem.* **2006**, *16*, 45.
[36] T. Savenje, J. E. Kroeze, X. Yang, J. Loos, *Adv, Funct. Mater.* **2005**, *15*, 1260.
[37] V. D. Mihailetchi, H. Xie, B. de Boer, L. J. A. Koster, P. W. M. Blom, *Adv. Funct. Mater.* **2005**, *15*, 1260.
[38] J. Huang, G. Li, Y. Yang, *Appl. Phys. Lett.* **2005**, *87*, 112105.
[39] A. Pivrikas, G. Juska, A. J. Mozer, M. Scharber, K. Arlauskas, N. S. Sariciftci, H. Stubb, R. Österbacka, *Phys. Rev. Lett.* **2005**, *94*, 176806.
[40] X. Ai, M. C. Beard, K. P. Knutsen, S. E. Shaheen, G. Rumbles, R. J. Ellingson, *J. Phys. Chem. B* **2006**, *110*, 25462.
[41] T. Erb, U. Zhokhavets, G. Gobsch, S. Raleva, B. Stühn, P. Schilinsky, C. Waldauf, C. J. Brabec, *Adv. Func. Mater.* **2005**, *15*, 1193.
[42] P. Schilinsky, U. Asawapirom, U. Scherf, M. Biele, C. J. Brabec, *Chem. Mater.* **2005**, *17*, 2175.
[43] a) J. Kline, M. D. McGehee, E. N. Kadnikova, J. Liu, J. M. J. Fréchet, *Adv. Funct. Mater.* **2003**, *15*, 1519. b) A. Zen, J. Pflaum, S. Hirschmann, W. Zhuang, F. Jaiser, U. Asawapirom, J. P. Rabe, U. Scherf, D. Neher, *Adv.*

Funct. Mater. **2004**, *14*, 757. c) J. Kline, M. D. McGehee, E. N. Kadnikova, J. Liu, J. M. J. Fréchet, M. F. Toney, *Macromol.* **2005**, *38*, 3312.

[44] R. C. Hiors, R. de Bettignies, J. Leroy, S. Bailly, M. Firon, C. Sentein, A. Khoukh, H. Preud'homme, C. Dagron-Lartigau, *Adv. Funct. Mater.* **2006**, *16*, 2263.

[45] W. Ma, J. Y. Kim, K. Lee, A. J. Heeger, *Macromol. Rapid Commun.* **2007**, *28*, 1776.

[46] a) H. Sirringhaus, P. J. Brown, R. H. Friend, M. M. Nielsen, K. Bechgaard, B. M. W. Langeveld-Voss, A. J. H. Spiering, R. A. J. Janssen, E. W. Meijer, P. Herwig, D. M. de Leeuw, *Nature* **1999**, *401*, 685. b) X. Jiang, R. Patil, Y. Harima, J. Ohshita, A. Kunai, *J. Phys. Chem. B* **2005**, *109*, 221.

[47] G. Li, Y. Yao, H. Yang, V. Shrotriya, G. Yang, Y. Yang, *Adv. Funct. Mater.* **2007**, *17*, 1636.

[48] V. D. Mihailetchi, H. Xie, B. de Boer, L. M. Popescu, J. C. Hummelen, P. W. M. Blom, J. J. A. Koster, *Appl. Phys. Lett.* **2006**, *89*, 012107.

[49] J. Peet, C. Soci, R. C. Coffin, T. Q. Nguyen, A. Mihailovsky, D. Moses, G. C. Bazan, *Appl. Phys. Lett.* **2006**, *89*, 252105.

[50] W. Wang, H. Wu, C. Yang, C. Luo, Y. Zhang, J. Chen, Y. Cao, *Appl. Phys. Lett.* **2007**, *90*, 183512.

[51] a) K. Landfester, *Macromol. Rapid Commun.* **2001**, *22*, 896. b) K. Landfester, *Adv. Mater.* **2001**, *13*, 765.

[52] K. Landfester, R. Montenegro, U. Scherf, R. Günter, U. Asawapirom, S. Patil, D. Neher, T. Kietzke, *Adv. Mater.* **2002**, *14*, 651.

[53] T. Piok, S. Gamerith, C. Gadermaier, H. Plank, F. P. Wenzl, S. Patil, R. Montenegro, T. Kietzke, D. Neher, U. Scherf, L. Landfester, E. J. W. List, *Adv. Mater.* **2003**, *15*, 800.

[54] C. J. Brabec, Public annual report of the BMBF project EKOS, 03N2023A-E, Jülich, **2004**.

[55] M. M. Bouman, E. E. Havinga, R. A. J. Janssen, E. W. Meijer, *Mol. Cryst. Liq. Cryst. Sci. Technol. A* **1994**, *256*, 439.

[56] A. Moulé, K. Meerholz, *Adv. Mater.* **2008**, *20*, 240.

[57] S. Berson, R. De Bettignies, S. Bailly, S. Guillerez, *Adv. Funct. Mater.* **2007**, *17*, 1377.

[58] a) E. Mena-Osteritz, A. Meyer, B. M. W. Langeveld-Voss, R. A. J. Janssen, E. W. Meijer, P. Bäuerle, *Angew. Chem.* **2000**, *112*, 2792. b) S. Malik, A. K. Nanti, *J. Polym. Sci, Part B Polym. Phys.* **2002**, *40*, **2073**.

[59] L. J. A. Koster, V. D. Mihailetchi, P. W. M. Blom, *Appl. Phys. Lett.* **2006**, *88*, 093511.

[60] M. C. Scharber, D. Mühlbacher, M. Koppe, P. Denk, C. Waldauf, A. J. Heeger, C. J. Brabec, *Adv. Mat.* **2006**, *18*, 789.

[61] J.-L. Bredas, D. Beljonne, V. Coropceanu, J. Cornil, *Chem. Rev.* **2004**, *104*, 4971.

[62] C. J. Brabec, C. Winder, N. S. Sariciftci, J. C. Hummelen, A. Dhanabalan, P. A. van Hal, R. A. J. Janssen, *Adv. Funct. Mater.* **2002**, *12*, 709.

[63] J. Roncali, *Chem. Rev.* **1997**, *97*, 173.

[64] H. A. M. van Mullekom, J. A. J. M. Vekemans, E. E. Havinga, E. W. Meijer, *Mater. Sci. Eng.* **2001**, *32*, 1.

[65] L. H. Slooff, S. C. Veenstra, J. M. Kroon, D. J. D. Moet, J. Sweelssen, M. M. Koetse, *Appl. Phys. Lett.* **2007**, *90*, 143506.

[66] F. Zhang, W. Mammo, L. M. Andersson, S. Admassie, M. R. Andersson, O. Inganäs, *Adv. Mater.* **2006**, *18*, 216. 9.

[67] N. Blouin, A. Michaud, M. Leclerc, *Adv. Mater.* **2007**, *19*, 2295.

[68] D. Mühlbacher, M. Scharber, M. Morana, Z. Zhu, D. Waller, R. Gaudiana, C. J. Brabec, *Adv. Mater.* **2006**, *18*, 2884.

[69] M. M. Wienk, M. G. R. Turbiez, M. P. Struijk, M. Fonrodona, R. A. J. Janssen, *Appl. Phys. Lett.* **2006**, *88*, 153511.

[70] W.-Y. Wong, X.-Z. Wang, Z. He, A. B. Djurisic, C.-T. Yip, K.-Y. Cheung, H. Wang, C. S. K. Mak, W.-K. Chan, *Nat. Mater.* **2007**, *6*, 521.

[71] Q. Zhou, Q. Hou, L. Zheng, X. Deng, G. Yu, Y. Cao, *J. Appl. Phys.* **2004**, *84*, 1653.

[72] X. Wang, E. Perzon, F. Oswald, F. Langa, S. Admassie, M. R. Andersson, O. Inganäs, *Adv. Funct. Mater.* **2005**, *15*, 1665.

[73] S. Admassie, O. Inganäs, W. Mammo, E. Perzon, M. R. Andersson, *Synth. Met.* **2006**, *156*, 614.

[74] P.-L. T. Boudreault, A. Michaud, M. Leclerc, *Macromol. Rapid Commun.* **2007**, *28*, 2176.

[75] E. Wang, L. Wang, L. Lan, C. Luo, W. Zhuang, J. Peng, Y. Cao, *Appl. Phys. Lett.* **2008**, *92*, 333007.

[76] N. Blouin, A. Michaud, D. Gendron, S. Wakim, E. Blair, R. Neagu-Plesu, M. Belletete, G. Duricher, Y. Tao, M. Leclerc, *J. Am. Chem. Soc.* **2008**, *130*, 732.

[77] Z. Zhu, D. Waller, R. Gaudiana, M. Morana, D. Mühlbacher, M. Scharber, C. J. Brabec, *Macromol.* **2007**, *40*, **1981**.

[78] P. Coppo, M. L. Turner, *J. Mat. Chem* **2005**, *15*, 1123.

[79] A. Tsami, T. W. Bunnagel, T. Farrell, M. C. Scharber, S. A. Choulis, C. J. Brabec, U. Scherf, *J. Mater. Chem.* **2007**, *17*, 1353.

[80] M. Morana, M. Wegscheider, A. Bonanni, N. Kopidakis, S. Shaheen, M. Scharber, Z. Zhu, D. Waller, R. Gaudiana, C. J. Brabec, *Adv. Funct. Mater.* **2008**, *18*, 1757.

[81] M. Lenes, G.-J. A. H. Wetzelaer, F. B. Kooistra, S. C. Veenstra, J. C. Hummelen, P. W. M. Blom, *Adv. Mater.* **2008**, *20*, 2116.

[82] H. F. Wittmann, R. H. Friend, M. S. Khan, J. J. Lewis, *Chem. Phys.* **1994**, *101*, 2693.

[83] V. Marin, E. Holder, R. Hoogenbom, U. S. Schubert, *Chem. Soc. Rev.* **2007**, *36*, 618.

[84] A. J. Sandee, C. K. Williams, N. R. Evans, J. E. Davies, C. E. Boothby, A. Köhler, R. H. Friend, A. B. Holmes, *J. Am. Chem. Soc.* **2004**, *125*, 7041.

[85] B. Liang, L. Wang, Y. Xu, H. Shi, Y. Cao, *Adv. Funct. Mater.* **2007**, *17*, 3580.

[86] A. Kohler, H. F. Wittman, R. H. Friend, M. S. Khan, J. Lewis, *Synth. Met.* **1996**, *77*, 147.

[87] F. Guo, Y.-G. Kim, J. R. Reynolds, K. S. Schanze, *Chem. Commun.* **2006**, 1887.

[88] J. Gilot, M. M. Wienk, R. A. J. Janssen, *Nat. Mater.* **2007**, *6*, 704.

[89] W.-Y. Wong, X.-Z. Wang, Z. He, A. B. Djurisic, C.-T. Yip, K.-Y. Cheung, H. Wang, C. S. K. Mak, W.-K. Chan, *Nat. Mater.* **2007**, *6*, 704.

[90] H. Hoppe, S. Sariciftci, *Adv. Polym. Sci.* **2007**, *12*, 121.

[91] F. B. Kooistra, J. Knol, F. Kastenberg, L. M. Popescu, W. J. H. Verhees, J. M. Kroon, J. C. Hummelen, *Org. Lett.* **2007**, *9*, 551.

[92] C. J. Brabec, A. Cravino, D. Meissner, N. S. Sariciftci, T. Fromherz, M. T. Rispens, L. Sanchez, J. C. Hummelen, *Adv. Funct. Mater.* **2001**, *11*, 374.

[93] L. Zheng, Q. Zhou, X. Deng, M. Yuan, G. Yu, Y. Cao, *J. Phys. Chem. B* **2004**, *108*, 11921.

[94] P. Würfel, in *Physics of Solar Cells*, Wiley-VCH, Berlin, Germany **2004**.

[95] A. De Vos, *J. Phys. D. Appl. Phys.* **1980**, *13*, 839.

[96] a) M. A. Green, K. Emery, Y. Hisikawa, W. Warta, *Prog. Photovolt. Res. Appl.* **2007**, *15*, 425. b) M. Wanlass, P. Ahrenkiel, D. Albin, J. Carapella, A. Duda, K. Emery, D. Firedman, J. Geisz, K. Jones, A. Kibbler, J. Kiehl, S. Kurtz, W. McMahon, T. Moriarty, J. Olson, A. Ptak, M. Romero, S. Ward, 4th World Conference on Photovoltaic Energy Conversion (WCEP-4), Hawaii, May **2006**, pp 729.

[97] M. Hiramoto, M. Suezaki, M. Yokoyama, *Chem. Lett.* **1990**, 327.

[98] A. Yakimov, S. R. Forrest, *Appl. Phys. Lett.* **2002**, *80*, 1667.

[99] J. Xue, S. Ushida, B. P. Rand, S. T. Forrest, *Appl. Phys. Lett.* **2004**, *85*, 5757.

[100] B. Maennig, J. Drechsel, D. Gebeyehu, P. Simon, F. Kozlowski, A. Werner, F. Li, S. Grundmann, S. Sonntag, M. Koch, K. Leo, M. Pfeiffer, H. Hoppe, D. Meissner, N. S. Sariciftci, I. Riedel, V. Dyakonov, J. Parisi, *Appl. Phys. A* **2004**, *79*, 1.

[101] J. Drechsel, B. Maennig, K. Kozlowski, M. Pfeiffer, K. Leo, *Appl. Phys. Lett.* **2005**, *86*, 244 102.

[102] a) K. Triyana, T. Yasuda, K. Fujita, T. Tsutsui, *Thin Solid Films* **2005**, *477*, 198. b) K. Triyana, T. Yasuda, K. Fujita, T. Tsutsui, Jpn, J. Appl, Phys, **2004**, *43*, 2352. c) D. Cheyns, H. Gommans, M. Odijk, J. Poortmans, P. Heremans, *Sol. Energy Mater. Sol. Cells* **2007**, *91*, 399.

[103] G. Dennler, M. C. Scharber, T. Ameri, P. Denk, K. Forberich, C. Waldauf, C. J. Brabec, *Adv. Mater.* **2008**, *20*, 579.

[104] K. Kawano, N. Ito, T. Nishimori, J. Sakai, *Appl. Phys. Lett.* **2006**, *88*, 73514.
[105] G. Dennler, H.-J. Prall, R. Koeppe, M. Egginger, R. Autengruber, N. S. Sariciftci, *Appl. Phys. Lett.* **2006**, *89*, 73502.
[106] a) A. Colsmann, J. Junge, C. Kayser, U. Lemmer, *Appl. Phys. Lett.* **2006**, *89*, 203 506. b) A. G. F. Janssen, T. Riedl, S. Hamwi, H.-H. Johannes, W. Kowalsky, *Appl. Phys. Lett.* **2007**, *91*, 073519.
[107] A. Hadipour, B. de Boer, J. Wildeman, F. B. Kooistra, J. C. Hummelen, M. G. R. Turbiez, M. M. Wienk, R. A. J. Janssen, P. W. M. Blom, *Adv. Funct. Mater.* **2006**, *16*, 1897.
[108] J. Gilot, M. M. Wienk, R. A. J. Janssen, *Appl. Phys. Lett.* **2007**, *90*, 143512.
[109] W. J. E. Beek, M. M. Wienk, M. Kemerink, X. Yang, R. A. J. Janssen, *J. Phys. Chem. B* **2005**, *109*, 9505.
[110] G. Dennler, K. Forberich, T. Ameri, C. Waldauf, P. Denk, C. J. Brabec, K. Hingerl, A. J. Heeger, *J. Appl. Phys.* **2007**, *102*, 123109.
[111] V. Shrotriya, E. Hsing-En, G. Li, Y. Yao, Y. Yang, *Appl. Phys. Lett.* **2006**, *88*, 064104.
[112] N.-K. Persson, O. Inganäs, *Sol. Energy. Mater. Sol. Cells* **2006**, *90*, 3491.
[113] A. Hadipour, B. de Boer, P. W. M. Blom, *J. Appl. Phys.* **2007**, *102*, 074506.
[114] K. Tvingstedt, V. Andersson, F. Zhang, O. Inganäs, *Appl. Phys. Lett.* **2007**, *91*, 123514.
[115] G. Dennler, K. Forberich, M. C. Scharber, C. J. Brabec, I. Tomis, K. Hingerl, T. Fromherz, *J. Appl. Phys.* **2007**, *102*, 054 516.
[116] A. Cravino, *Appl. Phys. Lett.* **2007**, *91*, 243502.
[117] X. Wang, E. Perzon, J. L. Delgado, P. de la Cruz, F. Zhang, F. Langa, M. Anderson, O. Inganäs, *Appl. Phys. Lett.* **2004**, *85*, 5081.
[118] M. D. Irwin, D. B. Buchholz, A. W. Hains, R. P. H. Chang, T. J. Marks, *PNAS*, **2008**, *105*, 2783.
[119] T. Markvart, European Summer University: Energy for Europe, Strasbourg, 7–14 July **2002**.
[120] G. Dennler, C. J. Brabec, in *Organic Photovoltaics: Materials, Device Physics, and Manufacturing Technologies* (Eds: C. J. Brabec, U. Scherf, V. Dyakonov), Wiley-VCH, Weinheim **2008**.
[121] K. Zweibel, in *Thin Film Solar Cells* (Eds: J. Poortmans, V. Arkhipov), Wiley-VCH, Berlin, Germany **2006**.